MAPPING WATER ICE CLOUD MICROPHYSICS WITH OMEGA/MEX.

J.-B. Madeleine *(jbmlmd@lmd.jussieu.fr)*, **F. Forget, A. Spiga,** *Laboratoire de Météorologie Dynamique, Institut Pierre Simon Laplace, Paris, France,* **J.-P. Bibring, B. Gondet, D. Jouglet, M. Vincendon, Y. Langevin, F. Poulet,** *IAS, Orsay, France,* **F. Montmessin,** *Service d'Aéronomie, Institut Pierre Simon Laplace, Paris, France,* **B. Schmitt,** *Laboratoire de Planétologie de Grenoble, France.*

Introduction:

Near-IR hyper-spectral imaging of clouds is currently used on Earth as a powerful meteorological tool, and this technique is made possible on Mars by the OMEGA (Observatoire pour la Minéralogie, l'Eau, les Glaces et l'Activité, [1]) imaging spectrometer.

Past analyses of clouds have been done in the visible range with Mariner 9 and Viking Orbiter [2], and more recently in the visible (MOC images [3]) and thermal infrared (TES, 6 to 50 µm [4,5]) with Mars Global Surveyor. Bridging the gap, OMEGA data are spectral image cubes (x,λ,y) of the atmosphere and the surface both in the visible and near infrared, spanning 0.35 to 5.1 µm with a spectral sampling of 0.013-0.020 µm and kilometer-scale spatial resolution. Spectral range includes water ice absorption bands at 1.25, 1.5, 2 and 3 µm that can be used to detect water-ice clouds and derive their microphysical properties.

Analyzing the kilometer-scale microphysics of clouds on Mars is key to understanding their formation, their role in the water cycle and radiative transfer of the planet, their interaction with the dust cycle, and can provide major insights into the fundamental physics of nucleation.

Cloud cover mapping:

Radiance is corrected from the gaseous CO_2 and H_2O absorption bands through a simplified method described in [6]. Two spectral criteria are used to detect and map the cloud distribution using RGB composition:

- the red is proportional to the 3.4/3.525 µm criterion defined in [7] that uses the wing of the 3 µm H_2O vibration band ;
- the green is proportional to the absorption depth of the 1.5 µm water ice band (used in [8]) :

$$D_{1.5\mu m} = \sqrt{\frac{I_\lambda(1.5\mu m)I_\lambda(1.515\mu m)}{I_\lambda(1.3\mu m)I_\lambda(1.715\mu m)}}$$

- the blue is held constant.

Correlated decrease of both 1.5 and 3.4 µm criteria reveals the formation of water ice clouds, and appears in blue. On the contrary, large 1.5 µm absorption and saturation of the 3 µm band are typical of surface grains larger than 10 µm which appear in magenta, allowing us to distinguish between surface frost and clouds in polar regions (see Fig. 2).

Cloud microphysical properties:

Cloud optical depth and particle size can be retrieved at a given point using an inversion method presented in Fig. 1. The model minimizes the difference between a simulated reflectance and the observed cloud reflectance by using a downhill simplex method and a least-squares criterion. The free parameters are the optical depth of the cloud at 3.2 µm τ_c and the water ice crystal effective radius r_e.

These two parameters are fitted during the inversion by calculating the radiative transfer through a single-layer atmosphere using the Spherical Harmonics Discrete Ordinate Method [9]. Scattering parameters are given by a Lorenz-Mie code which uses the recent ice optical constants at 180K of Grundy & Schmitt [10], and assumes that the ice crystals are spherical and follow a unimodal log-normal distribution (effective variance of 0.2).

A spectrum of the same region, free of any clouds, must be used as a surface boundary condition of the model. This spectrum must be carefully chosen through a "man-in-the-loop" method, in order to make sure that the surface geology, the atmospheric dust opacity and the viewing geometry are similar to what is found for the analyzed cloudy pixel.

Automatic imaging of the two microphysical parameters (r_e,τ_c) over an entire orbit is challenging and still under study.

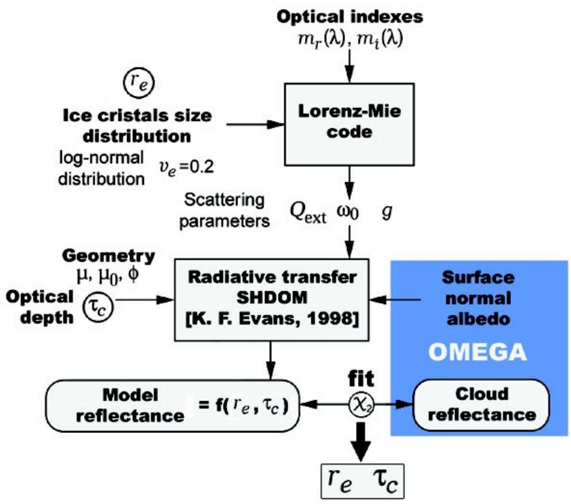

Figure 1. Schematic drawing of the water-ice crystals size r_e and cloud optical depth τ_c retrieval method.

Meteorological applications:

Polar regions. The different response of the 1.5 µm and 3 µm absorption bands to the ice particle size [7] is used in RGB compositions to distinguish between surface frost and clouds, as illustrated in Fig. 2. Seasonal frost appears in magenta around 76°N, and on the rim of a crater, whereas spring clouds appear in blue at the margin of these deposits.

Equatorial Cloud Belt. Evolution of the Aphelion Cloud Belt is characterized by an early period of cloud development (hazes and fibrous clouds) during Ls=45-130°, and convective cloud formation during Ls=80-130° [2,3]. An example of thick hazes surrounding Pavonis Mons is shown in Fig. 3 (upper panels), and inversion results (r_e = 3 µm, τ_c = 3.4) are consistent with TES EPF observations [5] and GCM results [11]. Ice crystal effective radius is found to reach 6 µm in convective regions.

Future work:

Improvements of the inversion model are underway to take into account the retrieval uncertainties, the radiative effect of atmospheric dust [12] and ice nucleation on mineral dust cores, the contribution of the 3 µm hydration band of surface dust [13], and to quantitatively map the microphysical properties over an entire orbit. Final results from the inversion model will be compared to the water cycle simulated by the LMD/GCM [11], and regional cloud structures will be interpreted with the help of the new LMD mesoscale model [14].

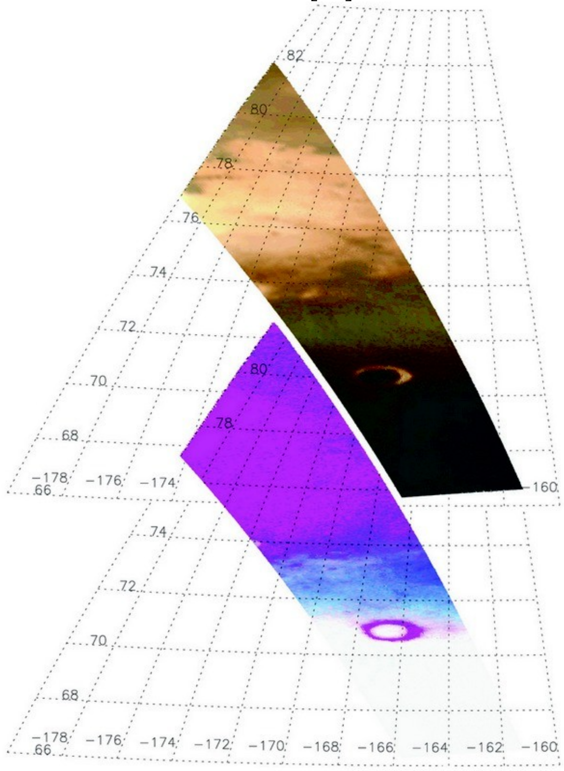

Figure 2. Water-ice frost and clouds in the northern polar region (visible and false-color compositions, ORB3064_3, Ls=59.4°, 75.1N-168.2W).

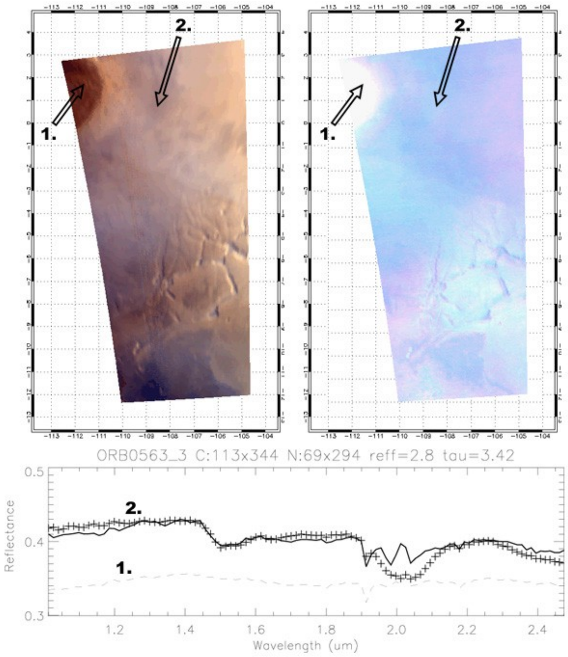

Figure 3. *Upper panels:* Mapping of thick hazes over Noctis Labyrinthus (visible and false-color compositions, ORB0563_3, Ls=53.6°, 8:30AM). *Lower panel:* Best fit found at the end of the inversion process, over a spectral range of 1.1 to 2.4 µm (r_e = 3 µm, τ_c = 3.4).

References:

[1] Bibring, J.-P. et al. *(2005), Science 307.* [2] Kahn, R. *(1984), JGR 89.* [3] Wang, H. and Ingersoll, A. P. *(2002), JGR 107.* [4] Smith, M. D. *(2004), Icarus 167.* [5] Clancy, R. T. et al. *(2003), JGR 108.* [6] Erard, S. and Calvin, W. *(1997), Icarus 130.* [7] Langevin, Y. et al. *(2006), JGR 112:E8.*
[8] Gondet, B. et al. *(2006), AGU, Abs. #P14A-02.* [9] Evans, K. F. *(1998), J. Atmos. Sci. 55.* [10] Grundy, W. M. and Schmitt, B. *(1998), JGR 103.* [11] Montmessin, F. et al. *(2004), JGR 109:E18.* [12] Vincendon, M. et al. *(2007), JGR 112:E11.* [13] Jouglet, D. et al. *(2007), JGR 112:E11.* [14] Spiga, A. et al. *(2008), MWCW, this issue.*